ARTICLE

Incorporation of Reactive Corrosion Inhibitor in Waterborne Acrylic Polyurethane Coatings and Evaluation of its Corrosion Performance

Lin Gu[a*], Ji-heng Ding[a,b], Shuan Liu[a], Hai-bin Yu[a*]

a. Key Laboratory of Marine Materials and Related Technologies, Zhejiang Key Laboratory of Marine Materials and Protective Technologies, Ningbo Institute of Materials Technology and Engineering, Chinese Academy of Sciences, Ningbo 315201, China
b. School of Chemical Engineering, Nanjing University of Science and Technology, Nanjing 210094, China

Hydroxyl-epoxy phosphate (HEP) as a reactive corrosion inhibitor was innovatively synthesized by the reaction of bisphenol A epoxy resin with phosphoric acid. HEP was mixed with hydroxyl acrylate resin, and crosslinked with waterborne isocyanate curing agent, which was used to form waterborne HEP/acrylic polyurethane composite (HEP-APU) coatings on Q235 steel surfaces. Electrochemical impedance spectroscopy and polarization curves were applied to analyze the corrosion behavior of the HEP-APU coatings in 3.5wt% NaCl solutions. The results indicated that the HEP-APU coatings show a superior passivation property and efficient corrosion protection of Q235 steel. The waterborne acrylic polyurethane coating containing 0.5wt% HEP exhibited the best corrosion performance among all the coating specimens. The improved flash-rust resistance can be attributed to the introduction of the phosphate group which could form phosphate film on the steel substrate.

Key words: Hydroxyl-epoxy phosphate, Acrylic polyurethane, Electrochemical impedance spectroscopy, Corrosion performance, Passivation

I. INTRODUCTION

In recent decades, waterborne coating materials have gained more and more concerns under the enormous environmental pressures [1, 2]. Waterborne coatings have been extensively used in the fields of architecture and furniture, but their applications in metal protection are still limited [3]. It is well known that hydrophilic groups or surfactants are necessary to impart the dispersion stability in aqueous media to waterborne resins [4]. However, these hydrophilic components are considered to form polar channels that will accelerate the water permeation and water uptake, and deteriorate the corrosion resistance [5]. Therefore, waterborne coatings commonly have some shortcomings, such as poor resistance to water, weak adhesion, and flash-rust, which limit their further applications in metal protection.

Adhesion and flash-rust resistance could be significantly improved by phosphating of metal [6] or adding the phosphating agents in coatings as fillers [7, 8]. However, these methods are not environment-friendly due to the use of toxic heavy metals. An alternative strategy is to incorporate organic phosphate group into polymer chains [9]. It has been reported that several commercial phosphate-type acrylates such as Sipomer® or Phosmer® monomers were easily incorporated into polymer systems via emulsion polymerization, and strongly enhanced adhesive and corrosion protective properties [9, 10]. Zhong et al. synthesized a styrene-acrylic emulsion containing phosphate acrylate monomer and hydroxylpropyl acrylate as crosslinking monomer, and found that the adhesion and flash-rust resistance of the emulsion on the metal substrate can be effectively improved by adding a phosphate monomer [11]. Li et al. used the reactive emulsifier with phosphate functional groups to synthesize an acrylate emulsion, where the phosphate group reacted with the metal surface to form the phosphate film, and then improved the adhesion of the coating to the metal and flash-rust resistance of the emulsion [12]. However, except for phosphate acrylate compounds, there is still lack of enough investigation into other phosphate-type compounds for the same purpose.

In this work, a new corrosion inhibitor, hydroxyl-epoxy phosphate (HEP), was successfully synthesized by the reaction of bisphenol A epoxy resins with phosphoric acids. The reactive HEP was easily incorporated into waterborne acrylic polyurethane (APU) systems. The anticorrosive properties of the APU films with various HEP were evaluated by electrochemical impedance spectroscopy (EIS), polarization curves and flash-rust

*Authors to whom correspondence should be addressed. E-mail: gulin1985@gmail.com, haibinyu@nimte.ac.cn, Tel.: +86-574-87911126

resistance.

II. EXPERIMENTS

A. Materials

Bisphenol A epoxy resin E44 was purchased from Hong Kong Honour Rich Decoration Material International Group Limited. Waterborne hydroxyl acrylate resin (Neocyl XK-110) was provided by DSM. Its hydroxyl content and solid content is 0.55wt% and 46.5wt%, respectively. Waterborne curing agent (XH-5008, NCO%, 20wt%−22wt%) was provided by Dongguan City Xuyihua Chemical Industry Limited Company. Phosphoric acid (85wt%), *N*,*N*-dimethyl ethanolamine and acetone were purchased from Alddin Industrial Corporation. All chemicals were used as received.

The Q235 steel was sealed with cured epoxy resin to leave an exposed geometrical surface area of 1.0 cm^2 as a working electrode. The exposed surfaces were gradually polished with SiC abrasive paper from 150 grit to 1200 grit, and then degreased ultrasonically in acetone, finally dried with nitrogen.

B. Synthesis of hydroxyl-epoxy phosphate (HEP)

A solution of bisphenol A epoxy resin E44 (20 g, in 40 mL acetone) was added dropwise into a phosphoric acid solution (9.22 g phosphoric acid in 20 mL acetone, the molar ratio of phosphoric acid to epoxy group is 1:1) under vigorously stirring at 30 °C in 30 min, the mixture was then vigorously stirred until the acid value remains constant (97.23 mg KOH/g). After that, *N*,*N*-dimethyl ethanolamine (11.27 g) and water were added dropwise into the mixture. Upon completion of the reaction, the solvent acetone was removed using a rotary vacuum evaporator, and then a transparent emulsion was obtained. The hydroxyl value and solid content of the emulsion is 2.53 mmol/g and 50wt% according to ASTM D 7253:2006 and D 6980-04, respectively.

C. Preparation of the HEP/acrylic polyurethane coatings

Different amounts of hydroxyl-epoxy phosphate were mixed with waterborne hydroxyl acrylate resins. Based on NCO/OH molar ratio 1:1, a calculated amount of waterborne curing agent was added. The mixture was stirred magnetically for 10 min. The liquid coatings were applied on the Q235 steel electrode surfaces with a bar coater, and then the specimens were baked in a vacuum oven at 60 °C for 30 min. The coating thickness was 80±2 μm measured using a PosiTector6000FNS1 apparatus. Coated samples were referred as APU, 0.2-P, 0.5-P and 1.0-P, according to the wt% of HEP in the solid content of coatings (0%, 0.2%, 0.5% and 1.0%, respectively).

D. Characterizations

^{1}H NMR spectra were recorded at room temperature on a NMR spectrometer (400 MHz AVANCE III, Bruker) in deuterated chloroform with tetramethylsilane as internal reference. FTIR spectra were performed on a spectrometer (NICOLET 6700, Thermo) by collecting 32 scans at a spectral resolution of 4 cm^{-1}. The acetone solutions of the samples were cast onto a KBr table and allowed to evaporate at room temperature. The fractured surfaces of the HEP-APU coatings were examined using a scanning electron microscope (SEM, FEI Quanta FEG 250). Flash-rust test was carried out according to the standard conditions (temperature 23 °C, humidity 50±5%, time 24 h).

The anticorrosive performance of the coating on Q235 steel in the 3.5wt% NaCl aqueous solution was evaluated on a CHI-660E electrochemical system. The electrochemical tests were conducted in a classical three-electrode cell system with a HEP-APU coating/Q235 steel as the working electrode, a saturated calomel electrode (SCE) equipped with a Luggin capillary as the reference electrode and a platinum plate of 2.5 cm^2 as the counter electrode. Before EIS measurement, the working electrode was immersed in the same solution for 2 h under open circuit potential (OCP) until a stable state was attained (the OCP fluctuation was less than ±5 mV). For EIS, the test frequency range was $10^5 - 10^{-2}$ Hz and the amplitude of the sinusoidal voltage signal was 20 mV. EIS data were analyzed by ZsimpWin 3.21 software. Polarization curves were recorded from −200 mV to +200 mV versus OCP by changing the electrode potential automatically with a scan rate of 0.5 mV/s.

III. RESULTS AND DISCUSSION

A. Synthesis and characterization of hydroxyl-epoxy phosphate

HEP was prepared by the reaction of bisphenol A epoxy resins with phosphoric acids, followed by neutralization with *N*,*N*-dimethyl ethanolamine and dilution with water, as shown in Scheme 1.

FTIR and ^{1}H NMR spectra were used to characterize the obtained HEP. Figure 1 shows FTIR spectra of the bisphenol A epoxy resin (E44) and HEP. The sharp absorption peaks at 1609, 1575 and 1512 cm^{-1} are assigned to stretching vibrations of the phenyl ring. The peaks at 3482 and 1049 cm^{-1} belong to stretching vibrations of the -OH and C−O−C groups, respectively. As can be seen from Fig.1(b), the sharp absorption peak at 911 cm^{-1} characteristic of epoxide groups disappears
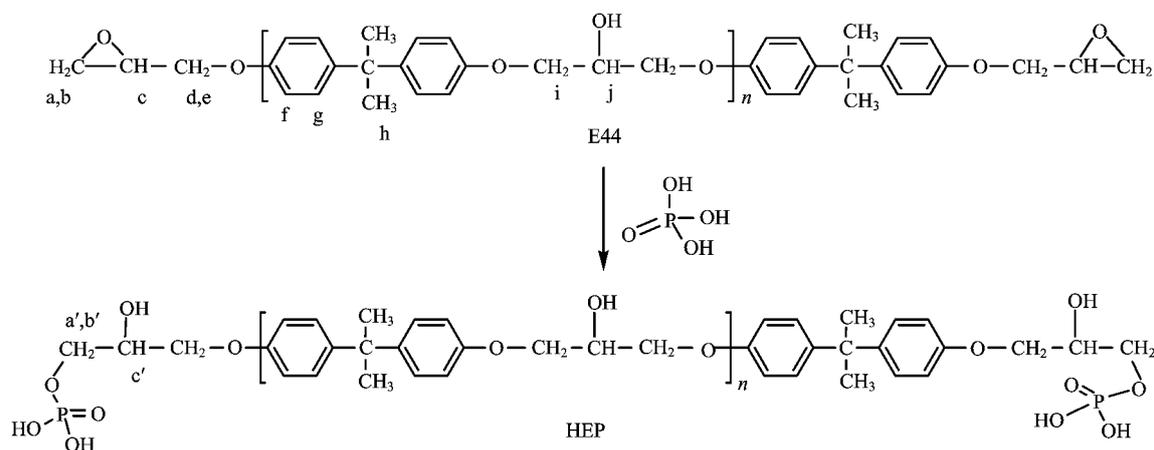
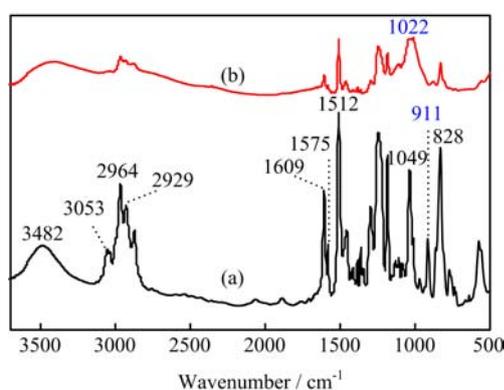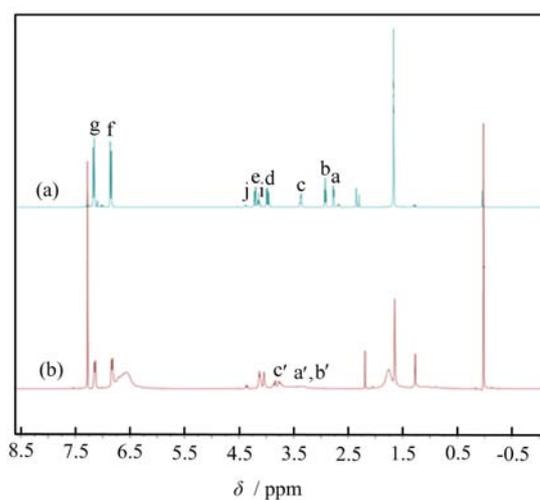Scheme 1 Synthetic route for the preparation of hydroxyl-epoxy phosphate.

FIG. 1 FTIR spectra of bisphenol A epoxy resin E44 (a) and hydroxyl-epoxy phosphate HEP (b).

FIG. 2 ^{1}H NMR spectra of bisphenol A epoxy resin E44 and hydroxyl-epoxy phosphate. The a−g and a′−c′ positions were shown in Scheme 1.

and the new peak at 1022 cm^{-1} characteristic of phosphate groups is observed, indicating that the reaction of epoxide groups and phosphoric acid was complete [13].

Figure 2 shows ^{1}H NMR spectra of E44 and HEP. The signals at 2.77 and 2.92 ppm are assigned to CH$_2$ in epoxide groups, while the signals at 3.37 ppm are assigned to CH in epoxide groups (Fig.2(a)) [13, 14]. However, these signals have totally disappeared in Fig.2(b) for HEP, which further demonstrates that a reaction has occurred between the epoxide groups in E44 and the phosphoric acid.

## B. Anticorrosion performance of the HEP-APU coatings

As shown in Scheme 2, waterborne acrylic polyurethane coatings containing HEP (HEP-APU) were prepared by mixing hydroxyl acrylate resin and HEP, followed by crosslinking with waterborne isocyanate curing agent.

The fractured surfaces of APU and HEP-APU coat-

ings with different contents of HEP were examined using SEM, as shown in Fig.3. From SEM images, the thickness of the coatings could be estimated to be 80−100 μm. The cross-section morphologies of these coatings were very similar, and all of them were rough and dense.

EIS is a powerful tool to analyze the corrosion protection mechanism of the coatings [15]. To investigate the anticorrosive performance of the HEP-APU coatings with different contents of HEP (APU, 0.2-P, 0.5-P and 1.0-P), the Nyquist and Bode plots of these four different coatings in 3.5wt% NaCl solution under different immersion time are presented in Fig.4.

The impedance modulus at a low frequency represents the ability of the coating to impede the flow of current between anodic and cathodic areas, which is in-
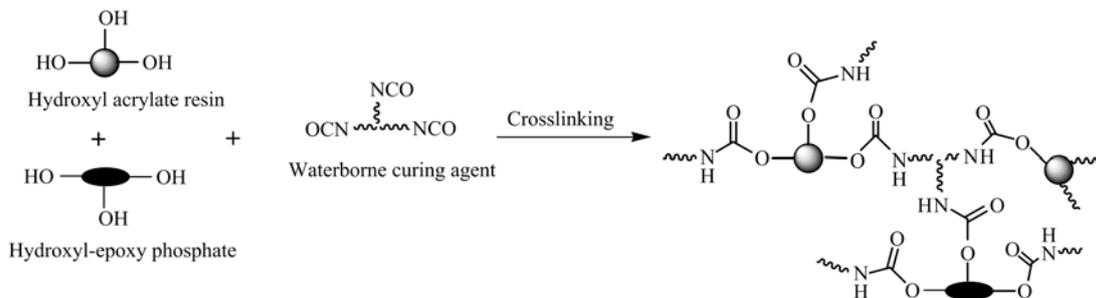
Scheme 2 Synthetic route for the preparation of waterborne acrylic polyurethane coatings containing HEP.
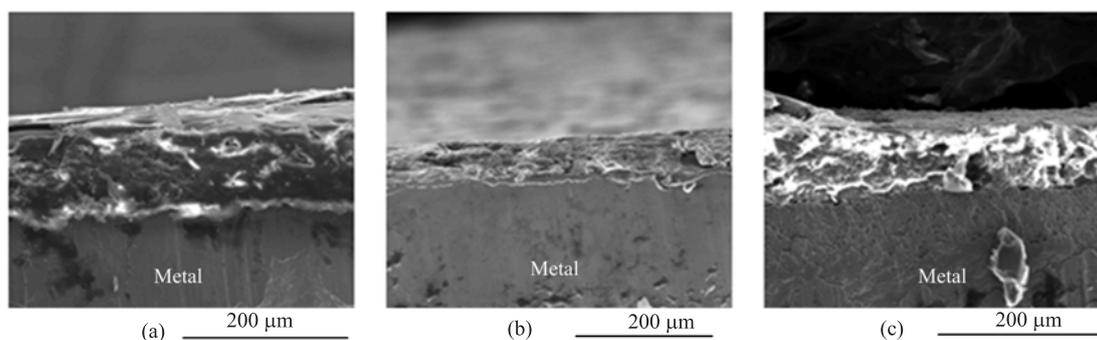

FIG. 3 SEM images of fractured surfaces of APU (a) and the HEP-APU coatings with different contents of HEP ((b) 0.5-P and (c) 1.0-P).

versely proportional to corrosion rate [16, 17]. It can be seen that the 0.5-P coated Q235 steel showed the best corrosion protection performance with the impedance modulus value of about 3.8×10^4 $\Omega \cdot cm^2$ at 10^{-2} Hz after 48 h. For the APU coating, the impedance modulus decreased rapidly during the first 12 h of immersion, and then remained stable. For the HEP-APU coatings, the impedance modulus decreased gradually with time during the immersion. Compared with the APU coating, the impedance module values of 0.2-P and 0.5-P were much higher. These results indicated that the addition of HEP improved the anticorrosion performance of the APU coating.

The peak at different frequency ranges in the Bode plots represents different time constants. For the HEP-APU coatings, two time constants occurred during the all immersion times. The Nyquist plots exhibited a capacitive arc at a high frequency corresponding to coating resistance (R_c) and coating capacitance (Q_c), and a bigger capacitive arc at the medium-low frequency corresponding to double layer capacitor (Q_{dl}) and charge transfer resistance (R_{ct}), respectively [18].

For quantitative estimatation the evolution of barrier and active anticorrosion properties of the HEP-APU coating systems, EIS data were fitted with equivalent circuit R(Q(R(QR))), as shown in Fig.5. The equation used for the fitting of the EIS results is presented as Eq.(1):

$$Z = R_s + \cfrac{1}{j\omega Q_c + \cfrac{1}{R_c + \cfrac{1}{j\omega Q_{dl} + \cfrac{1}{R_{ct}}}}} \quad (1)$$

In this study, constant phase element, Q, instead of capacitance was used in all fittings, because the coating may exhibit heterogeneous nature due to the presence of pores [19, 20]. Q is expressed as:

$$Q = \frac{1}{Y_0 \omega^n} \cdot \left(\cos \frac{n\pi}{2} + j \sin \frac{n\pi}{2} \right) \quad (2)$$

where Y_0 and n are the constant and exponent, respectively, and ω is the angular frequency in rad/s ($\omega = 2\pi f$), and $j^2 = -1$ is an imaginary number. When $n=1$, Q represents a capacitance C, for $n=0$, Q represents a resistance R, for $n=0.5$, a diffusion impedance and for $n=-1$, Q represents an inductance L. Generally, if $0.5<n<1.0$, it corresponds to capacitance response, if $0.1<n<0.5$, an intermediate phenomenon (diffusion impedance) occurs [21]. R_s represents the solution resistance, and Q_c and R_c represent the coating capacitance and coating resistance, respectively. Q_{dl} and R_{ct} represent the double-layer capacitance and charge-transfer resistance, respectively.
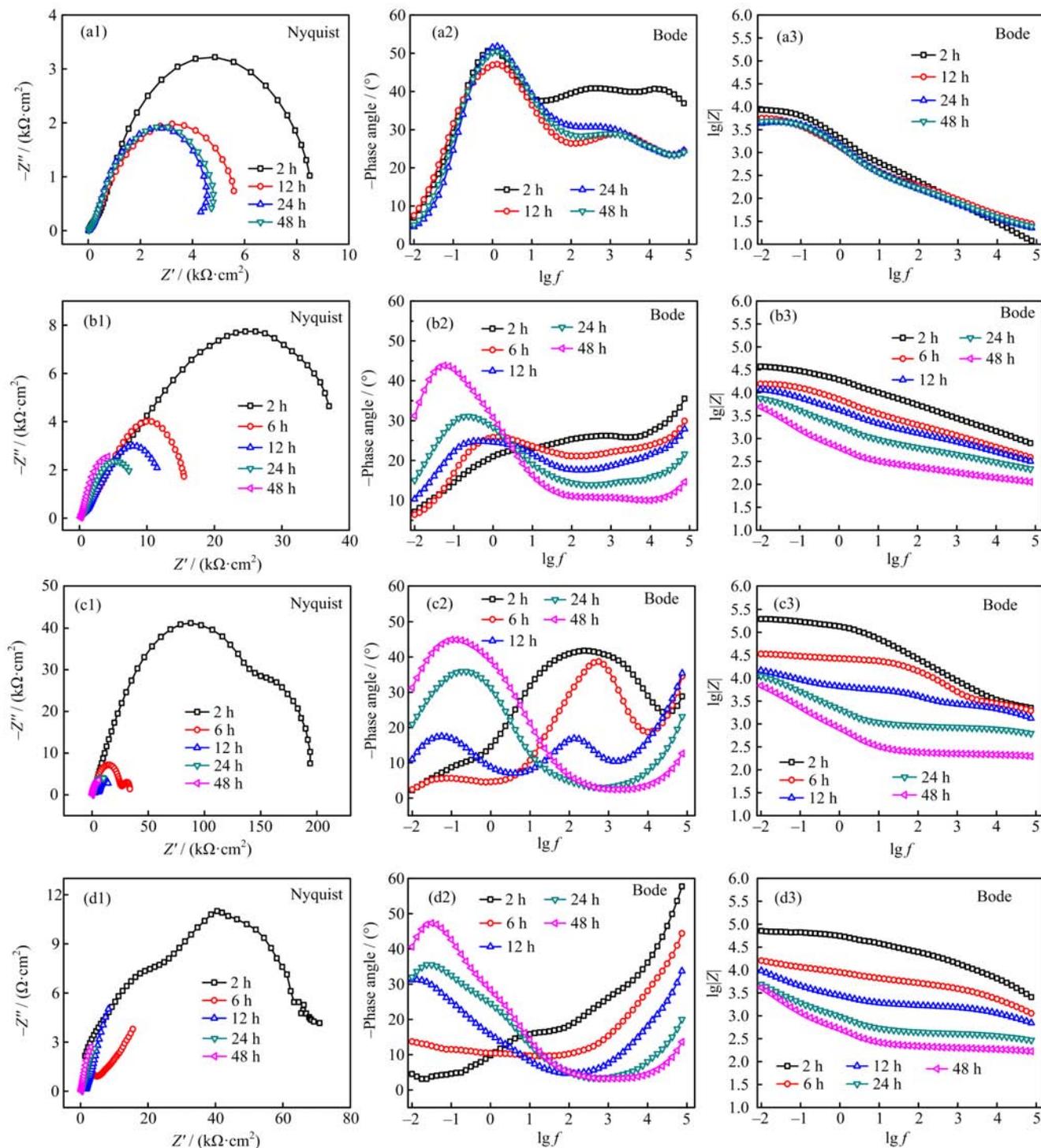
FIG. 4 Nyquist and Bode plots of HEP-APU coating/Q235 steel system with different contents of HEP under different immersion time in 3.5wt% NaCl solution: (a) APU, (b) 0.2-P, (c) 0.5-P, (d) 1.0-P.

The results of the fitting corrosion parameters are listed in Table I. The resistance and capacitance of the HEP-APU coatings depend on the compactness of the coating, its crack ability and amount of absorbed water. It should be note that for 0.2-P coating, the n_1 values were ranged from 0.32 to 0.38 between 6 and 48 h immersions, indicating that a diffusion response but not capacitive response occurred in the middle-high frequency region because some "dispersion effects" (such as water penetration) led to deviation from the
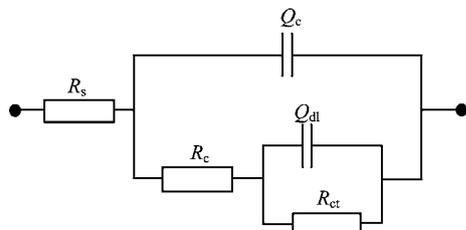
FIG. 5 Equivalent circuits used to fit the EIS data of HEP-APU coatings/Q235 steel system in 3.5wt% NaCl solution.

TABLE I The fitting parameters of HEP-APU coating/Q235 steel system in 3.5wt% NaCl solution under different immersion time (time in h, R_s and R_c in $\Omega \cdot cm^2$, Q_c in $\mu FHz^{1-n_1}/cm^2$, Q_{dl} in $\mu FHz^{1-n_2}/cm^2$, R_{ct} in $k\Omega \cdot cm^2$).

	Time	R_s	Q_c	n_1	R_c	Q_{dl}	n_2	R_{ct}
APU	2	0.01	110	0.54	876.2	35.2	0.94	9.897
	12	0.01	360	0.41	329.1	182	0.79	4.447
	24	0.01	190	0.48	239.5	221	0.72	4.982
	48	0.01	210	0.52	189.4	265	0.68	4.015
0.2-P	2	0.01	0.082	0.69	886	19.7	0.36	50.8
	6	0.01	25.1	0.37	310.6	27.2	0.59	16.9
	12	0.01	37.5	0.33	175.4	74.7	0.51	15.5
	24	0.01	83.1	0.32	80.4	170	0.56	13.1
	48	0.01	180	0.38	21.2	642	0.59	10.5
0.5-P	2	0.01	1.05	0.55	18300	15.6	0.99	274
	6	0.01	7.74	0.24	2790	43.5	0.76	193
	12	0.01	3.63	0.79	3601	250	0.63	124
	24	0.01	1.27	0.66	850.1	231	0.59	106
	48	0.01	4.59	0.77	217.5	538	0.61	116
1.0-P	2	0.01	3.91	0.61	21000	0.52	0.91	81.2
	6	0.01	0.231	0.62	3644	11.2	0.27	36.5
	12	0.01	6.64	0.56	1603	382	0.42	25.3
	24	0.01	3.23	0.65	376.1	720	0.47	10.1
	48	0.01	6.65	0.59	197.8	998	0.54	9.79

FIG. 6 Evolution of R_c and R_{ct} with immersion time for modified APU containing different contents of HEP in 3.5wt% NaCl solution.

capacitance response.

For all coatings, Q_c and Q_{dl} increased with time because of the water uptake [19, 22]. To further analyze the coating deterioration processes, R_c and R_{ct} of the different HEP-APU coatings were shown in Fig.6, respectively, as a function of immersion time. A higher R_c implies a smaller number of H_2O and O_2 molecules penetrating into the coatings [23]. The R_c of the neat APU decreased from the initial value of 876.2 $\Omega \cdot cm^2$ to a steady value of about 189.4 $\Omega \cdot cm^2$ after 48 h immersion. For 0.5-P and 1.0-P, their values of R_c were much higher than that of the neat APU, but decreased rapidly with time and then maintained a stable state. With the water uptake and penetration of Cl^-, metal corrosion occurred in the interface between the coating and Q235
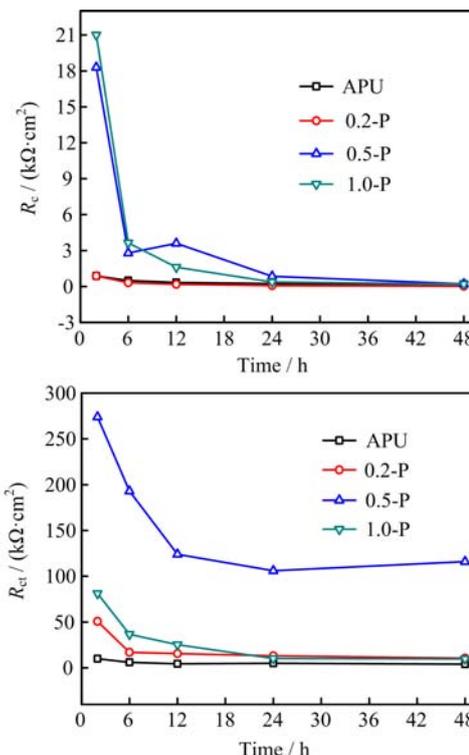
steel substrate. R_{ct} is a parameter of the resistance to electron transfer across a metal surface and is inversely proportional to the corrosion rate [24]. The R_{ct} of all coatings decreased during the first 24 h then remained stable in 3.5wt% NaCl solution. It is rather remarkable that the R_{ct} of the 0.5-P coating was about 100 k$\Omega \cdot cm^2$ after 48 h immersion, ~30 times higher than that the APU coating, indicating that this coating had some passivation properties and excellent protectiveness towards Q235 steel. In conclusion, the 0.5-P coating exhibited the best corrosion protection performance.

Figure 7(a) presented the polarization Tafel curves of the bare Q235 steel without and with APU and 0.5-P coatings immersed in 3.5wt% NaCl solution after 48 h. The cathodic branches of the polarization curves displayed a typical Tafel behavior, therefore, the corrosion density (i_{corr}) and corrosion potential (E_{corr}) were fitted from the extrapolation of the Tafel zone of the cathodic branch to the E_{corr} and then summarized in Table II [25, 26]. Compared with the bare Q235 steel, the polarization curves of the Q235 steel with the APU coating shifted towards nobler potentials and lower current densities, indicating that the APU coating improved the corrosion resistance of the Q235 steel. Furthermore, the 0.5-P coated Q235 steel had a negative corrosion potential (−0.683 V) but a lower corrosion current density (0.625 $\mu A/cm^2$) than that of the APU coating.
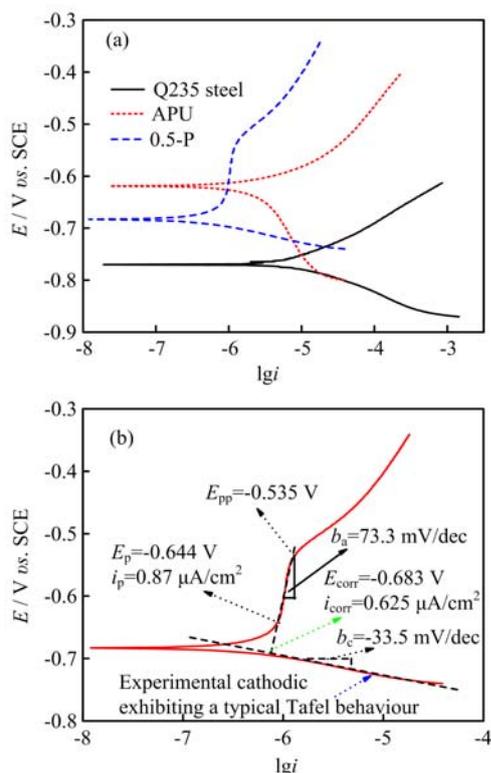
FIG. 7 (a) The Tafel curves recorded for the Q235 steel, APU and 0.5-P coatings immersed in 3.5wt%NaCl solution after 48 h, (b) a cathodic and anodic polarization curve plot obtained for 0.5-P coating in 3.5wt%NaCl solution, representing calculations of the various corrosion parameters associated with polarization measurements.

TABLE II Electrochemical parameters of HEP-APU coatings on Q235 steel immersed in 3.5wt% NaCl solution after 24 h.

Specimens	E_{corr}/V $vs.$ SCE	i_{corr}/(μA/cm^2)
Q235	-0.769	2.381
APU	-0.621	0.897
0.5-P	-0.683	0.625

To elucidate the effect of HEP as in an inhibiting film in the HEP-APU coating, the cathodic and anodic polarization curve plot obtained for 0.5-P coatings in 3.5wt% NaCl solution is showed in Fig.7(b), and the corrosion parameters was marked. Obviously, Q235 steel was in the passivative state when it was coated with HEP-APU coatings. The passive potential range was from -0.644 V to -0.535 V, and the passivation current density (i_{p}) was 0.87 μA/cm^2. The slope of anodic polarization curve b_{a} (73.3 mV/dec) was much higher than b_{c} (-33.5 mV/dec), suggesting that HEP was an anodic inhibitor in APU coating for carbon steel protection [27].
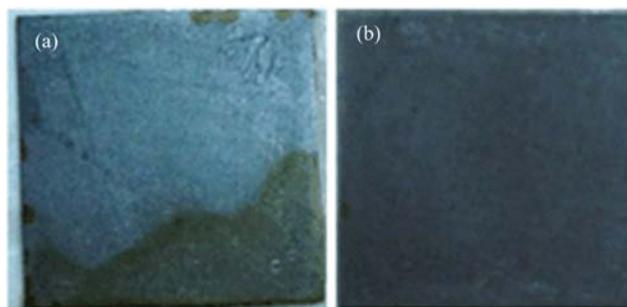

FIG. 8 Flash-rust on steel of (a) APU coatings and (b) APU coatings with 0.5wt% HEP.
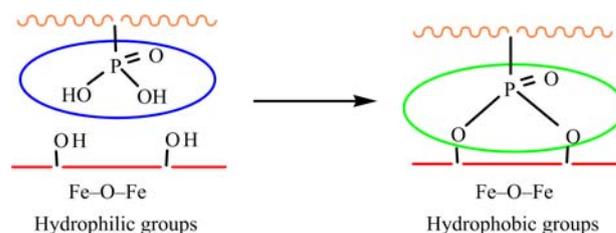

FIG. 9 Schematic illustration of the anticorrosive mechanism of the HEP-APU films with phosphate functional groups.

Furthermore, the forming of phosphate film could improve the flash-rust resistance property of APU film on the steel substrate. As is shown in Fig.8, the substrate coated with 0.5-P had no flash-rust, while the steel substrate coated with the APU was rusted seriously. The reason is that the phosphate functional group could anchor on the metal surface with covalent bonds which turned the hydrophilic groups into the hydrophobic groups (Fig.9). Therefore, the HEP acts as the crosslinking bridge between the APU film and metal surface.

IV. CONCLUSION

A new reactive corrosion inhibitor HEP was synthesized by the reaction of bisphenol A epoxy resins with phosphoric acids. The HEP was easily incorporated into waterborne APU systems by mixing hydroxyl acrylate resin with HEP, followed by crosslinking with waterborne isocyanate curing agent. The anticorrosive properties of the APU film with HEP in 3.5wt% NaCl solution were evaluated by EIS, polarization curves and flash-rust resistance. The flash-rust resistance was improved due to the introduction of the phosphate group which could form phosphate film on the steel substrate. A superior passivation property by the HEP-APU coating was also observed. The waterborne APU coating containing 0.5wt% HEP exhibited the best corrosion performance among all the coating specimens.

V. ACKNOWLEDGMENTS

[1] C. Fu, T. X. Zhang, C. Q. Ji, F. Cheng, W. Z. Cui, and Y. Chen, Chin. J. Polym. Sci., **33**, 14 (2015).
[2] C. W. Lai, Y. Sun, H. Yang, X. Q. Zhang, and B. P. Lin, Acta Chim. Sin. **71**, 1201 (2013).
[3] M. Liu, X. H. Mao, H. Zhu, A. Lin, and D. H. Wang, Corros. Sci. **75**, 106 (2013).
[4] M. Hirose, J. Zhou, and K. Nagai, Prog. Org. Coat. **38**, 34 (2000).
[5] J. Taylor and M. Winnik, J. Coat. Technol. Res. **1**, 163 (2004).
[6] T. Yu and C. T. Lin, Ind. Eng. Chem. Res. **36**, 368 (1997).
[7] C. T. Lin, Prog. Org. Coat. **42**, 226 (2001).
[8] H. Neuder, C. Sizemore, M. Kolody, R. Chiang, and C. T. Lin, Prog. Org. Coat. **47**, 225 (2003).
[9] I. González, D. Mestach, J. R. Leiza, and J. M. Asua, Prog. Org. Coat. **61**, 38 (2008).
[10] H. S. Yang, H. Adam, and J. Kiplinger, JCT Coat. Technol. **2**, 44 (2005).
[11] Z. Zhong, Q. Yu, H. Yao, W. Wu, W. Feng, L. Yu, and Z. Xu, Prog. Org. Coat. **76**, 858 (2013).
[12] Y. F. Li, J. J. Zhu, X. H. Gao, and Z. M. Yu, J. Macromol. Sci. A **50**, 248 (2013).
[13] Y. Liu, C. Zhang, Z. Du, and H. Li, J. Appl. Polym. Sci. **99**, 858 (2006).
[14] L. Gu, Y. Qin, Y. Gao, X. Wang, and F. Wang, J. Polym. Sci. Part A **51**, 2834 (2013).
[15] C. Liu, Q. Bi, and A. Matthews, Corros. Sci. **43**, 1953 (2001).
[16] L. Gu, S. Liu, H. Zhao, and H. Yu, RSC Adv. **5**, 56011 (2015).
[17] T. T. Hang, T. A. Truc, N. T. Duong, N. Pébère, and M. G. Olivier, Prog. Org. Coat. **74**, 343 (2012).
[18] S. Liu, H. Sun, N. Zhang, and L. Sun, Int. J. Corros. **2013**, 1 (2013).
[19] H. Y. Sun, S. Liu, and L. J. Sun, Int. J. Electrochem. Sci. **8**, 3494 (2013).
[20] S. Liu, H. Sun, L. Sun, and H. Fan, Corros. Sci. **65**, 520 (2012).
[21] F. Alcaide, E. Brillas, and P. L. Cabot, J. Electroanal. Chem. **547**, 61 (2003).
[22] L. Gu, S. Liu, H. Zhao, and H. Yu, ACS Appl. Mater. Interfaces **7**, 17641 (2015).
[23] Y. Zhang, Y. Shao, T. Zhang, G. Meng, and F. Wang, Prog. Org. Coat. **76**, 804 (2013).
[24] H. Wei, D. Ding, S. Wei, and Z. Guo, J. Mater. Chem. A **1**, 10805 (2013).
[25] C. Y. Tsai, J. S. Liu, P. L. Chen, and C. S. Lin, Surf. Coat. Tech. **205**, 5124 (2011).
[26] M. A. Amin, K. F. Khaled, and S. A. Fadl-Allah, Corros. Sci. **52**, 140 (2010).
[27] B. Qian, J. Wang, M. Zheng, and B. Hou, Corros. Sci. **75**, 184 (2013).